Research Article

Journal of PeptideScience

Received: 20 June 2011 Revised: 31 August 2011 Accepted: 9 September 2011 Published online in Wiley Online Library

(wileyonlinelibrary.com) DOI 10.1002/psc.1423

Synthesis and NMR elucidation of novel tetrapeptides

Maya Makatini,[a] Thashini Chetty,[b] Oluseye K. Onajole,[b] Thavendran Govender,[a] Patrick Govender,[c] Glenn E. M. Maguire[b] and Hendrik G. Kruger[b]*

The synthesis and NMR elucidation of Ala-Val-Pro-Ile and five novel peptide-based derivatives are reported. These peptides mimic the natural second mitochondria-derived activator of caspase (Smac) protein. Purification was achieved using preparative HPLC and the NMR elucidation of all compounds is reported for the first time. A series of overlapping signals were observed in the 1D NMR spectra thus making assignment a difficult task to undertake. The use of 2D NMR techniques with the inclusion of efficient adiabatic symmetrized ROESY proved to be an effective tool in overcoming these difficulties. Copyright © 2011 European Peptide Society and John Wiley & Sons, Ltd.

Supporting information may be found in the online version of this article.

Keywords: polycyclic 'cage'; AVPI; 2D NMR

Introduction

Cancer amongst other diseases such as heart disease and stroke has recently been widely acknowledged as a leading cause of death in the US [1]. Statistics released by the World Health Organization revealed that patient numbers will increase to 16 million new cases per annum by 2020 [1]. In South Africa, recent statistics reveal that one in six men and one in seven women will develop cancer in their lifetimes [1].

Apoptosis refers to the biochemical, molecular and physiological processes that are involved in programmed cell death and was initially coined by Kerr and co-workers [2]. Apoptosis is required in controlled embryonic development, such as in the formation of hands and feet by the removal of the webbing between the digits and for the maintenance of cellular homeostasis of an organism [3–5]. Problems with the regulation of apoptosis can lead to diseases such as cancer, Parkinson's, Alzheimer's, preeclampsia and various autoimmune diseases [6]. In cancer cells, one of the protein functions that could be malfunctioning is apoptosis. The X-chromosome-linked inhibitor of apoptosis protein (XIAP) is therefore an attractive strategy to potentially combat cancer [7].

The aim of this study was to prepare peptides that mimic the natural second mitochondria-derived activator of caspase (Smac) protein, which has the amino acid sequence Ala-Val-Pro-Ile (AVPI). It was proposed that these compounds would inhibit the IAPs by binding to the baculovirus IAP repeat 2 and 3 domains present at the amino terminus of XIAP and, in doing so, promote apoptosis in cancer cells [7]. Researchers over the years have explored the structure–activity relationship of the parent compound (AVPI) in the bid to either enhance its activity or make it more lipophilic to aid cell permeability [8]. Four synthetic strategies were employed in this study, namely, *N*-methylation, Pro substitution by tetrahydroisoquinoline (TIQ), L-hydroxyproline and incorporation of cage amino acids into the peptide sequence. We recently reported the synthesis and complete NMR elucidation of pentacycloundecane-based peptides on the basis of these same principles (AVPI) [9]. The cage amino acids were shown to exhibit β-turn characteristics comparable with that of Pro [10]. Cage compounds are also known to cross cell membranes as well as crossing the blood–brain barrier and the CNS [11–13].

Herein, we report the structural analysis of the synthetic products utilizing 2D NMR spectroscopic techniques.

Chemistry

The active Smac *N*-terminal tetrapeptide NH_2-AVPI-$CONH_2$ (Figure 1 (**1**)) was synthesized using both manual and automated SPPS techniques. Rink amide resin was chosen for the synthesis to yield an amide terminal on Ile upon cleavage from the resin. The manual SPPS of *N*-methylated AVPI (**2**) containing *N*-methylations at the Ala, Val and Ile residues was unsuccessful. The synthesis was repeated numerous times while varying synthetic strategies such as coupling reagents, coupling times, deprotection and cleavage methods with no success. The target peptide, however was successfully synthesised using a microwave automated peptide

* *Correspondence to: Hendrik G. Kruger, School of Chemistry, University of KwaZulu-Natal, Durban 4001, South Africa. E-mail: kruger@ukzn.ac.za*

a *School of Pharmacy and Pharmacology, University of KwaZulu-Natal, Durban 4001, South Africa*

b *School of Chemistry, University of KwaZulu-Natal, Durban 4001, South Africa*

c *School of Biochemistry, Genetics and Microbiology, University of KwaZulu-Natal, Durban, South Africa*

Journal of PeptideScience

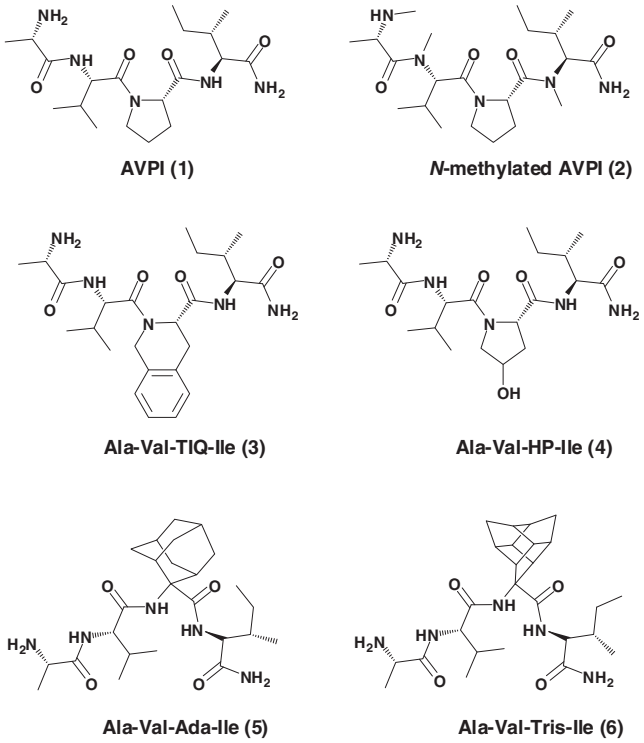

Figure 1. Structure of AVPI and AVPI analogues.

synthesizer and purified via semipreparative HPLC using a water/acetonitrile solvent system.

Proline was substituted in the AVPI sequence with TIQ (peptide **3**). This compound was also synthesized using both manual and automated SPPS techniques. Both techniques yielded the desired compound as the major product. A by-product with $m/z = 361.3$ was also observed in which the Val residue had not coupled completely to the TIQ amino acid probably because of steric hindrance. The effect of 4-hydroxyproline replacing Pro in the NH_2-AVPI sequence were also investigated. Prior to use in the peptide synthesis, the amino group of 4-hydroxyproline was protected using Fmoc after which normal coupling procedures were carried out to acquire the desired peptide **4** without any by-products (Figure 1).

The starting materials adamantane amino acid [11] and trishomocubane amino acid [14–16] were synthesized from 2-adamantanone and trishomocubanone. Both 'cage' amino acids were Fmoc protected prior to use [9]. The 'cage' amino acids were used as a substitute for Pro in the synthesis of the AVPI tetrapeptide to obtain peptides **5** and **6**. The automated microwave SPPS was employed to incorporate the 'cage' structure into the peptide sequence on a rink amide resin.

Results and Discussions

Structural elucidation of peptides prepared in this study was carried out using 2D NMR techniques. This information in combination with the data obtained from high-resolution MS serves to confirm the successful synthesis of the target peptides.

Heteronuclear multiple bond coherence (HMBC) and NOESY or ROESY are valuable techniques to cross-link the various signals of amino acid residues of the peptide structures.

A disappointing observation was that few through-space NOE interactions were observed for these peptides, even with the use of efficient adiabatic symmetrized (EASY) ROESY. Low temperature NMR experiments (down to $-15\,^{\circ}C$) also did not improve the situation, confirming the flexible nature of these short peptides.

There are at least four useful points of entry for the elucidation of the NMR spectra of peptide **1** (AVPI) (Figure 1). The HMBC interaction of the Ala methyl protons (H-1) with the carbonyl carbon (C-3), the characteristic methyl protons (H-22/H-23) of the Val fork [17], the Pro α-hydrogen (H-11), which is the only possible triplet (it could potentially also be a pair of doublets because H-10 is diastereotopic) and the characteristic ethyl group on Ile.

For brevity, detailed discussion of the assignments for the peptides will not be presented here but is provided with the supporting information. The NMR data for AVPI (**1**) and peptide **2** (*N*-methylated AVPI) are presented in Table 1.

Upon comparison of the heteronuclear single quantum coherence (HSQC) spectrum of peptide **1** (blue and green) and **2** (red) (Figure 2), three distinct methyl signals at 3.03, 2.94 and 2.67 p.p.m. were observed. These signals can be assigned to the *N*-methyl groups present.

The starting point for elucidation of peptide **3** (Ala-Val-TIQ-Ile) was the two fully substituted carbons on the aromatic ring (C-26 and C-31). The carbon spectrum of the compound shows six aromatic carbon signals between 125.0 and 135.0 p.p.m. Of these, the two resonances at 134.5 and 134.7 p.p.m. corresponds to the quaternary carbons C-26 and C-31. The assignments for Ala-Val-TIQ-Ile are presented in Table 2.

Table 1. ^{1}H and ^{13}C NMR data for AVPI (**1**) and *N*-methylated AVPI (**2**)

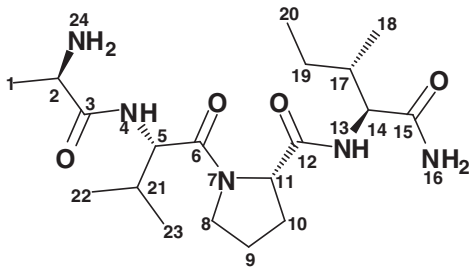

1

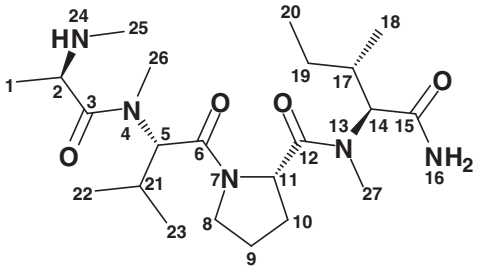

2

AVPI (**1**)				*N*-methylated AVPI (**2**)			
Atom	$\delta^{1}H^{a,b}$	*J* (Hz)	$\delta^{13}C^{a,b}$	Atom	$\delta^{1}H^{a,b}$	*J* (Hz)	$\delta^{13}C^{a,b}$
1	1.30		17.8	1	1.18		16.0
2	3.92		48.4	2	5.01		55.6
3	—		169.8	3	—		167.0
4	8.54		—	4	7.22		—
5	4.37		56.4	5	4.92		59.2
6	—		169.7	6	—		171.7
7	—	—	—	7	—		—
8a	3.60	[c]	47.7	8a	3.55	[c]	46.9
8b	3.68	[c]	47.7	8b	3.61	[c]	46.9
9a	1.81	[c]	25.0	9a	1.98	[c]	24.4
9b	1.92	[c]	25.0	9b	1.78	[c]	24.4
10a	1.81	[c]	29.3	10a	1.66	[c]	28.1
10b	1.99	[c]	29.3	10b	2.18	[c]	28.1
11	4.42		59.6	11	4.71		56.4
12	—		171.7	12	—		171.8
13	7.70		—	13	7.29		—
14	4.10		57.1	14	4.61		59.0
15	—		173.3	15	—		170.8
16	7.00		—	16	6.91		—
17	1.68		37.4	17	1.92		31.5
18	0.84		15.9	18	0.84		15.2
19a	1.10	7.20	24.7	19a	1.39	[c]	24.0
19b	1.45	7.20	24.7	19b	0.99	[c]	24.0
20	0.81		11.6	20	0.79		10.1
21	1.99		30.9	21	2.16		26.4
22	0.90		18.5	22	0.78		18.4
23	0.93		18.1	23	0.90		19.9
24	8.05		—	24	7.64		—
				25	2.67		28.3
				26	3.03		30.1
				27	2.94		29.6

[a]600 MHz for ^{1}H and 150 MHz for ^{13}C.
[b]Solvent $(CD_3)_2SO_2$.
[c]Because of overlapping signals, the respective coupling constants could not be determined.

The next structure to be elucidated was peptide **4** (Ala-Val-HP-Ile). The only variation to the original structure is the replacement of one of the H-9 protons on Pro with a hydroxyl group. The Pro methylene protons (H-9) were observed at 1.81 and 1.92 p.p.m. (^{1}H spectrum) and 25.0 p.p.m. (^{13}C spectrum). By overlaying the HSQC spectrum of AVPI (blue and green) with that of the HP (red and pink) derivative, it is observed that the methylene proton signals for H-9 are absent (Figure 3).

The assignments for peptide **4** are presented in Table 2. The ^{13}C attached proton test (APT) spectrum was very useful in elucidating peptide **5**, the adamantane AVPI derivative. The numbering system for the adamantane cage is based on that proposed by Hickmott *et al.* in 1985 [18]. Only one quaternary carbon signal appears at 63.6 p.p.m., and it was assigned to C-2′. The amide proton, H-13 (7.56 p.p.m.), exhibits a NOESY interaction with a remaining methine signal, which could

Journal of PeptideScience

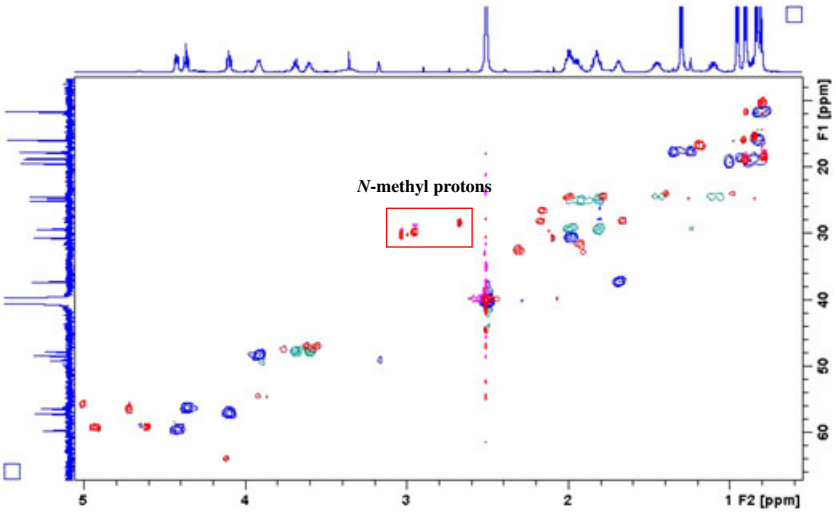

Figure 2. Overlay of the HSQC spectrum of peptide **1** (AVPI) (blue and green) and peptide **2** (red).

either be H-1′ or H-3′ of the adamantane cage. After the assignment of H-19a and H-19b (1.10 and 1.45 p.p.m.), the remaining methylene carbon resonances at 32.2 and 33.3 p.p.m. were assigned to the methylene protons of the cage (H-4′, H-6′, H-8′, H-9′ and H-10′). Peak overlapping made it impossible to further assign these protons. The assumed signal of H-1′/H-3′ and H-5′/H-7′ displayed both TOSCY and COSY interactions with all methylene protons appearing between 1.52–1.71 p.p.m. and 1.89–2.74 p.p.m., thus confirming the assignment of H-1′/H-3′ and H-5′/H-7′. A split signal is observed on the ^{13}C APT spectrum, i.e. two methine peaks overlap at 31.2 p.p.m., which is indicative of the overlapping of the H-1′/H-3′ and H-5′/H-7′ resonances. Unfortunately, further assignment cannot be carried out because of the extensive peak overlapping occurring from 1.52 to 1.71 p.p.m. and from 1.89 to 2.07 p.p.m.

The elucidation of the trishomocubane skeleton of peptide **6** has been reported before [14–16]. The only quaternary carbon in the structure of the trishomocubane derivative is C-4′. This signal was therefore assigned to the carbon at 69.7 p.p.m. because the other fully substituted carbon signals were present in the carbonyl region of the spectrum. From the ^{13}C APT spectrum, other CH_2 signals observed appear at 32.7, 31.9 and 24.1 p.p.m. The signal at 24.1 p.p.m. was already assigned to C-19 from the Ile residue; therefore, the remaining signals were assigned to C-7′ and/or C-11′ from the trishomocubane cage moiety. These carbon signals correspond to methylene protons at 1.35 and 1.31 p.p.m. in the HSQC spectrum. Splitting of these signals is observed with the other protons at 1.26 and 1.23 p.p.m., respectively.

The overlapping signals of H-7′ and H-11′ shows HMBC correlations with two carbon signals at 53.4 and 52.2 p.p.m. Looking at the structure, only two methine proton signals can appear at a higher frequency because of their chemical environment, namely H-3′ and H-5′. One would expect H-3′ to appear at a higher frequency because of the through-space deshielding effect contributed by the C-12 carbonyl, whereas H-5′ experiences a smaller deshielding effect from the C-6 carbonyl. With this assumption, the resonance at 2.58 p.p.m. was assigned to H-3′ and the other at 2.36 p.p.m. to H-5′. Further confirmation of these assignments was obtained from the ROESY spectrum. The H-7′ doublets display a ROESY correlation to two overlapping methine protons at 2.01 and 2.03 p.p.m., which were assigned to either H-6′ or H-8′. The proton resonances at 2.01 p.p.m. show a ROESY interaction to H-5′ and another signal at 2.08 p.p.m., whereas the second resonance at 2.03 p.p.m. shows a ROESY correlation to a signal at 2.40 p.p.m. and another at 2.48 p.p.m. The resonance at 2.01 p.p.m. was assigned to H-6′, whereas that at 2.08 p.p.m. was assigned to H-2′. Therefore, the signal at 2.03 p.p.m. was assigned to H-8′ by elimination. H-8′ displays a ROESY interaction with 2.09 and 2.48 p.p.m., which could be either H-1′ or H-9′. H-3′ shows a ROESY correlation with a signal at 2.07 p.p.m., which was assigned to H-10′, whereas a signal at 2.48 p.p.m. mentioned before shows a ROESY interaction to H-8′, H-11′ and another signal at 2.09 p.p.m. Therefore, 2.48 p.p.m. was assigned to H-9′, whereas that at 2.09 p.p.m. was assigned to H-1′. H-1′ shows ROESY correlations with the overlapping signals of H-7′ and H-11′ between 1.20 and 1.38 p.p.m. H-6′ and H-8′ show ROESY correlations to a proton at 1.35 p.p.m., which was assigned to H-7′. By elimination, H-11′ was assigned to 1.31 p.p.m. These protons are split (HSQC spectrum), and the second H-11′ proton resonates at 1.23 p.p.m. Similarly, the second proton of H-7′ was assigned to 1.25 p.p.m. The methine proton at 2.28 p.p.m. was assigned to H-2 by elimination. The relative trend observed for the trishomocubane carbon and proton chemical shifts are similar to that previously reported [14–16]. The corresponding carbon signals of all assigned protons of the trishomocubane AVPI derivative were assigned using the HSQC spectrum and are presented in Table 3.

Conclusion

The NMR elucidation of six peptides was successfully performed. Two-dimensional NMR spectroscopy was a vital tool in overcoming major overlapping observed with 1D NMR spectroscopy. No significant NOE interactions were observed for the family of peptides studied herein, even at low temperature. We have successfully utilized EASY ROESY [19] before in obtaining crucial information of the 3D solution structure of similar but

Table 2. ^{1}H and ^{13}C NMR data for peptides **3** and **4**

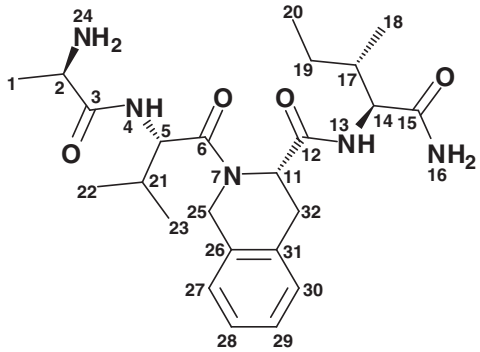

3

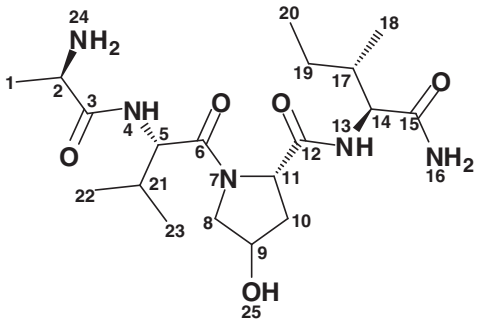

4

Ala-Val-TIQ-Ile (**3**)				Ala-Val-HP-Ile (**4**)			
Atom	$\delta^{1}H^{a,b}$	*J* (Hz)	$\delta^{13}C^{a,b}$	Atom	$\delta^{1}H^{a,b}$	*J* (Hz)	$\delta^{13}C^{a,b}$
1	1.16		20.5	1	1.23		21.2
2	3.48		49.8	2	3.48		50.2
3	—		173.22	3	—		171.5
4	7.31		—	4	8.10		—
5	4.06		57.08	5	4.45		55.1
6	—		171.0	6	—		173.4
7	—		—	7	—		—
11	4.38		54.1	8a	3.58	10.74	55.7
12	—		170.3	8b	3.70	10.50	55.7
13	7.53		—	9	4.39		69.1
14	4.81		54.1	10a	1.95	[c]	37.8
15	—		170.8	10b	2.05	[c]	37.8
16	7.51		—	11	4.55		58.8
17	2.09		31.3	12	—		
18	0.97		19.7	13	7.81		—
19a	0.92	[c]	24.2	14	4.15		57.1
19b	1.29	[c]	24.2	15	—		170.2
20	0.72		15.8	16	6.98		—
21	1.60		37.4	17	1.77		37
22	0.90		18.3	18	0.89		15.9
23	0.74		11.6	19a	1.18	[c]	24.6
24	7.02		—	19b	1.52	[c]	24.6
25	3.02		31.7	20	0.88		11.7
26	—		134.7	21	2.01		31.0
27	7.20		127.9	22	0.95		19.3
28	7.15/7.22		126.9/127.7	23	0.88		17.9
29	7.15/7.22		126.9/127.7	24	7,32		—
30	7.28		126.3	25	8.09		—
31	—		134.5				
32a	4.92	15.06	46.2				
32b	4.64	15.06	46.2				

[a]600 MHz for ^{1}H and 150 MHz for ^{13}C.
[b]Solvent $(CD_3)_2SO_2$.
[c]Because of overlapping signals, the respective coupling constants could not be determined.

Journal of PeptideScience

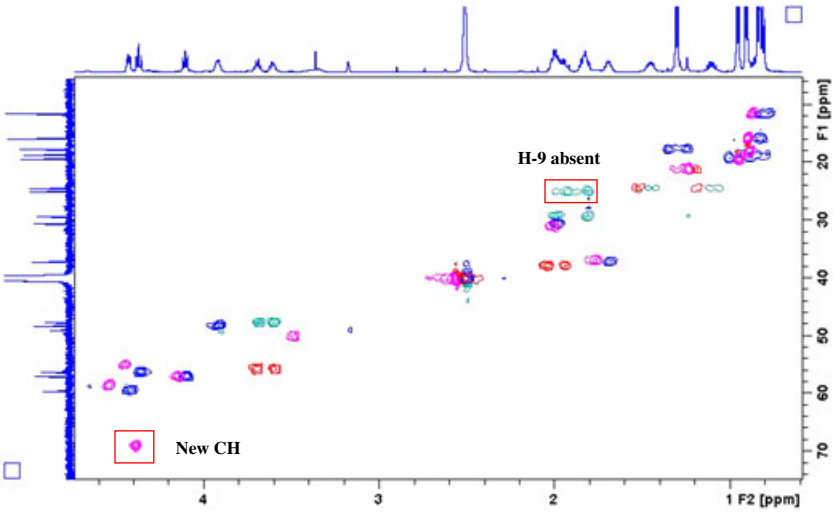

Figure 3. Overlay of the HSQC spectrum of peptide **1** (AVPI) (blue and green) and peptide **4** (HP) (pink and red) derivative of AVPI.

different short cage peptides [20]. This is an indication of the flexibility of AVPI peptides studied here.

Experimental Section

Detailed experimental information about the synthesis is presented in the supporting information of this manuscript.

The NMR spectra were recorded on a Bruker AVANCE III 400 and 600-MHz NMR spectrometers using Topspin 2.1 (Bruker, Karlsruhe, Germany). The chemical shifts were referenced to the solvent peak $\delta = 2.50$ p.p.m. (^{1}H) and 39.9 p.p.m. (^{13}C) for $(CD_3)_2SO$ at room temperature. The ^{1}H NMR spectra were recorded at a transmitter frequency of 600.100 MHz for peptides **1–4** and **6**. Peptide **1** was recorded with a spectral width of 7102.273 Hz, acquisition time of 2.307 s, pulse width of 15 μs, relaxation delay of 1.0 s and scans of 32. Peptides **2** and **4** were recorded with a spectral width of 12 335.526 Hz; acquisition time of 1.328 s; pulse width of 15 μs; relaxation delay of 1.0 s and scans of 8 and 16. Peptide **3** was recorded with a spectral width of 6849.315 Hz; acquisition time of 2.392 s; pulse width of 15 μs, relaxation delay of 1.0 s and scans of 16. Peptide **6** was recorded with a spectral width of 6203.473 Hz, acquisition time of 2.641 s, pulse width of 15 μs, relaxation delay of 1.0 s and scans of 16. All the previously presented data were obtained on a Bruker AVANCE III 600-MHz NMR instrument. The ^{1}H NMR spectra for peptide **5** was recorded at a transmitter frequency of 400.222 MHz (spectral width of 8223.685 Hz, acquisition time of 3.98 s, pulse width of 10 μs, scans of 16 and relaxation delay of 1.0 s) from the AVANCE III 400 MHz NMR instrument.

The ^{13}C NMR spectra for peptides **1**, **3** and **4** were recorded at 150.910 MHz with a spectral width of 36 057.69 Hz; acquisition time of 0.908 s; pulse width of 9.00 μs; relaxation delay of 2.00 s and scans of 16 000, 9600 and 13 312, respectively. All the previously presented data were obtained from the Bruker AVANCE III 600-MHz NMR instrument. The ^{13}C NMR spectra for peptide **2**, **5** and **6** were recorded at a transmitter frequency of 100.635 MHz with spectral width of 24 038.461 Hz, acquisition time of 1.363 s, pulse width of 8.40 μs, relaxation delay of 2.00 s and scans of 8192, 2048 and 4800, respectively, on the AVANCE III 400-MHz NMR instrument.

All 2D experimental data obtained on the Bruker AVANCE III 600 for peptides **1–4** and **6** were as follows: 90° pulse width of 15.1 μs for all spectra. Spectral widths for the ^{1}H spectra of peptide **1** are 7102.273 (COSY), 7075.475 (TOSCY), 6602.113 (ROESY) and 7102.273 Hz (HSQC and HMBC). Spectral widths for ^{1}H for peptide **2** are 12 335.526 (COSY), 6203.474 (TOSCY), 6009.615 (ROESY and HSQC) and 6203.474 Hz (HMBC). Spectral width for the ^{1}H spectra of peptide **3** is 6849.315 Hz for COSY, TOSCY, ROESY, HSQC and HMBC. Spectral widths for the ^{1}H spectra of peptide **4** are 12 335.526 (COSY) and 6203.474 Hz for TOSCY, NOESY, HSQC and HMBC. Spectral widths for the ^{1}H spectra of peptide **6** are 6203.474 Hz for COSY, TOSCY, HSQC and HMBC and 6009.615 Hz for NOESY.

All 2D experimental data obtained on the Bruker AVANCE III 400 for peptide **5** were as follows: 90° pulse width of 10 μs and spectral width for ^{1}H is 3937.008 Hz (COSY, TOSCY, NOESY, HSQC and HMBC).

The spectral widths for the ^{13}C spectra are 36 057.691 Hz (HSQC and HMBC) for **1**, 25 000, 33 557.047 Hz (HSQC and HMBC) for **2**, **4** and **6**, and 25 000, 36 057.691 Hz (HSQC and HMBC) for **3**; the number of data points per spectrum in F2 are 2048 (COSY), 2048 (TOSCY), 2048 (NOESY/ROESY), 4096 (HMBC) and 1024 (HSQC) for peptides **1–6**, whereas the number of time-incremented spectra in F1 were 128 (COSY), 256 (TOSCY), 256 (NOESY for **3–5**), 512 (ROESY for **1**, **2** and **6**), 128 (HMBC) and 256 (HSQC) for peptides **1–6**; relaxation delay for peptides **1** and **6** was 1.0 s for COSY, TOSCY, HSQC and HMBC spectra, whereas 2.0 s was used for the ROESY spectra. The relaxation delay for peptides **3** and **4** was 1.0 s for COSY, TOSCY, ROESY/NOESY, HSQC and HMBC spectra. The relaxation delay for peptide **2** was as follows: 1.0 s (COSY), 2.0 s (ROESY), 1.0 s (TOSCY), 2.5 s (HSQC) and 1.0 s (HMBC), whereas the relaxation delays for peptide **5** are 1.42 s (COSY), 1.99 s (NOESY and TOSCY), 1.46 s (HSQC) and 1.36 s (HMBC). The spectra acquired in phase-sensitive mode for all peptides are NOESY/ROESY and HSQC; the spectra for all peptides were acquired in absolute value mode. Gradients were used for the COSY, HSQC and HMBC spectra of all peptides. All NMR spectra are available as supporting information.

Table 3. ^{1}H and ^{13}C NMR data for peptides **5** and **6**

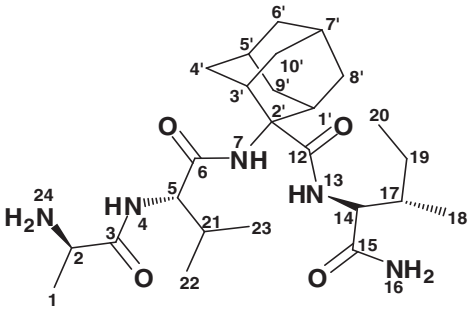

5

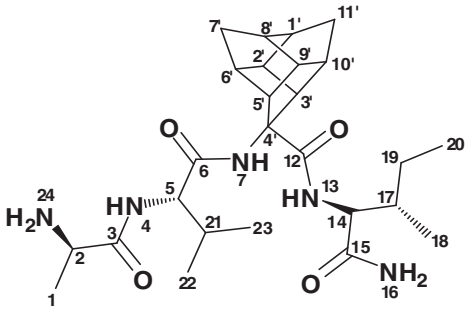

6

Ala-Val-Ada-Ile (**5**)				Ala-Val-Tris-Ile (**6**)			
Atom	$\delta^{1}H^{a,c}$	*J* (Hz)	$\delta^{13}C^{a,c}$	Atom	$\delta^{1}H^{b,c}$	*J* (Hz)	$\delta^{13}C^{b,c}$
1	0.87		11.3	1	0.93		19.4
2	1.78		26.3	2	2.28		43.9
3	—		171.3	3	—		171.2
4	8.30		—	4	8.13/8.15		—
5	4.31		57.6	5	4.20		57.8
6	—		173.6	6	—		172.8
7	7.32		—	7	7.36		—
12	—		172.9	12	—		172.9
13	7.56		—	13	7.36		—
14	4.19		56.7	14	4.10		56.7
15	—		171.6	15	—		171.6
16	8.00		—	16	7.00		—
17	1.77		37.0	17	1.80		36.9
18	0.88		15.5	18	0.88		15.6
19a	1.10	[d]	24.2	19a	1.10	[d]	24.2
19b	1.45	[d]	24.2	19b	1.40	[d]	24.2
20	0.86		11.3	20	0.88		11.2
21	2.01		30.7	21	1.98–2.05		30.5
22	0.91		17.9	22	0.90		17.9
23	0.92		19.4	23	0.91		18.3
24	7.00		—	24	7.86/7.88		—
2′	—		63.6	1′	2.09		41.8
1′ 3′ 5′ 7′	2.66–2.74		31.2	2′	2.08		42.7
4′ 6′ 8′ 9′ 10′	1.52–1.71		33.3	3′	2.58		52.2
4′ 6′ 8′ 9′ 10′	1.89–2.74		32.2	4′	—		69.7
				5′	2.36		53.4
				6′	2.01		43.0
				7′a	1.35	9.24	32.7
				7′b	1.25	9.84	32.7
				8′	2.03		42.1
				9′	2.48		53.1
				10′	2.07		42.7
				11′a	1.31	10.26	32.0
				11′b	1.23	10.38	32.0

[a]400 MHz for ^{1}H and 100 MHz for ^{13}C.
[b]600 MHz for ^{1}H and 150 MHz for ^{13}C.
[c]Solvent $(CD_3)_2SO_2$.
[d]Because of overlapping signals, the respective coupling constants could not be determined.

Acknowledgements

This study was supported by grants from the National Research Foundation, GUN 2073251, Aspen Pharmacare and the University of KwaZulu-Natal. We thank Dr Katja Petzold for assistance with the EASY ROESY experiments.

References

1 Bergman PJ. Radioresistance, chemoresistance and apoptosis resistance. The past, present and future. *Vet. Clin. North Am. Small Anim. Pract.* 1997; **27**: 47–57.
2 Kerr JF. Apoptosis: A basic biological phenomenon with wide-ranging implications in tissue kinetics. *Br. J. Cancer* 1972; **26**: 239–257.
3 Shi Y. A structural view of mitochondia-mediated apoptosis. *Nat. Struct. Biol.* 2001; **8**: 394–401.
4 Danial NN, Korsmeyer SJ. Cell death: critical control points. *Cell* 2004; **116**: 205–219.
5 Lowe SW, Lin AW. Apoptosis in cancer. *Carcinogenesis* 2000; **21**: 485–495.
6 Solary E. The role of apoptosis in the pathogenesis and treatment of diseases. *Eur. Respir. J.* 1996; **9**: 1293–1305.
7 Sun H, Nikolovska-Coleska Z, Yang CY, Qian D, Lu J, Qiu S, Bai L, Peng Y, Cai Q, Wang S. Design of small-molecule peptidic and nonpeptidic smac mimetics. *Acc. Chem. Res.* 2008; **41**: 1264–1277.
8 Letai A, Bassik MC, Walensky LD, Sorcinelli MD, Weiler S, Korsmeyer SJ. Distinct Bh3 domains either sensitize or activate mitochondrial apoptosis, serving as prototype cancer therapeutics. *Cancer Cell* 2002; **2**: 183–192.
9 Altaib MS, Arvidsson PI, Govender T, Maguire GEM, Makatini M, Onajole OK, Kruger HG. Synthesis and Nmr elucidation of novel pentacycloundecane-based peptides. *Magn. Reson. Chem.* 2010; **48**: 435–442.
10 Albericio F, Arvidson PI, Bisetty K, Giralt E, Govender T, Jail S, Kongsaeree P, Kruger HG, Prabpai S. Trishomocubane amino acid as a B-Turn scaffold. *Chem. Bio Drug Des.* 2008; **71**: 125–130.
11 Nagasawa HT, Elberling JA, Shirota FN. 2-aminoadamantane-2-carboxylic acid, a rigid, achiral, tricyclic a- amino acid with transport inhibitory properties. *J. Med. Chem.* 1973; **16**: 823–826.
12 Zah J, Terre'Blanche G, Erasmus E, Malan SF. Physicochemical prediction of a brain-blood distribution profile in polycyclic amines. *Bioorg. Med. Chem.* 2003; **11**: 3569–3578.
13 Geldenhuys WJ, Malan SF, Bloomquist JR, Marchand AP, Schyf CJV. *Med. Res. Rev.* 2005; **25**: 21–48.
14 Govender T, Kruger HG, Raasch T. Complete Nmr elucidation of two N-Protected trishomocubane hydantoins and the ethyl ester of the corresponding amino acid. *Struct. Chem.* 2005; **16**: 129–134.
15 Govender T, Hariprakasha HK, Kruger HG, Raasch T. Synthesis of trishomocubane amino acid derivatives. *S. Afr. J. Chem.* 2005; **58**: 37–40.
16 Fourie L, Govender T, Hariprakasha HK, Humcha K, Kruger HG, Raasch T. Complete Nmr elucidation of a novel trishomocubane hydantoin and its Mono- and Bis-T-Boc protected derivatives. *Magn. Reson. Chem.* 2004; **47**: 617–623.
17 Altaib MS, Arvidsson PI, Govender T, Maguire GEM, Makatini M, Onajole OK, Kruger HG. *Magn. Reson. Chem.* 2010; **48**(6): 435–442.
18 Hickmott PW, Wood S, Murray-Rust P. Introduction of pharmacophoric groups into polycyclic systems. Part 3. Amine derivatives of adamantane and diaza-adamantane. *Journal of Chemical Society Perkin Transactions I* 1985: 2033–2038.
19 Thiele CM, Petzold K, Schleucher J. Easy Roesy: Reliable cross-peak integration in adiabatic symmetrized roesy. *Chemistry-a European Journal* 2009; **15**: 585–588.
20 Makatini MM, Petzold K, Sriharsha SN, Soliman MES, Honarparvar B, Arvidsson PI, Sayed Y, Govender P, Maguire GEM, Kruger HG, Govender T. Pentacycloundecane-based inhibitors of wild-type c-south african hiv-protease. *Bioorganic & Medicinal Chemistry Letters* 2011; **21**: 2274–2277.

